RJC

RASĀYAN *J. Chem.*
Vol. 18 | No. 2 |788-796| April - June | 2025
ISSN: 0974-1496 | e-ISSN: 0976-0083 | CODEN: RJCABP
http://www.rasayanjournal.com
http://www.rasayanjournal.co.in

THE EFFECT OF PET AND EVA POLYMER MODIFICATION AS AGGREGATES IN THE PRODUCTION OF POLYMER MORTAR USING IMMERSION AND PRESSURE METHODS

Muhammad Amin[1,2], Ariadne Lakshmidevi Juwono[2,✉], Sudibyo[1], David Candra Birawidha[1], Sugeng Priyanto[3] and Muhammad Al Muttaqii[4]

[1]Research Center for Mining Technology, National Research and Innovation Agency (BRIN), South Lampung 35361, Indonesia

[2]Department of Physics, Faculty of Mathematics and Natural Science-University of Indonesia, Depok 16424, Indonesia

[3]Department of Mechanical Engineering, State University of Jakarta, East Jakarta 13220, Indonesia

[4]Research Center for Chemistry, National Research and Innovation Agency, Building 452 KST BJ Habibie, Serpong Tangerang Selatan 15314, Indonesia

✉Corresponding author: ariadne.laksmidevi@ui.ac.id

ABSTRACT

This paper investigates increasing polymer addition into ordinary cement mortar (OCM) composites. The main areas of study include material fabrication, workability, mechanical properties, durability, microstructure, and application of OCM composite materials. This paper introduces the application of PMCM and discusses the prospects and challenges of PMCM composite materials. In this work, we examine the impact of waste Ethylene Vinyl Acetate (EVA) and Polyethylene Terephthalate (PET) on cement-based mortar's mechanical characteristics and workability. Variations of 0.2%, 0.5%, 0.8%, 1.1%, and 1.4% of the PET polymer are employed in place of sand. In the meanwhile, variants of 2%, 4%, 6%, 8%, and 10% of the EVA polymer are used as Portland cement substitutes. Immersion techniques were used to create the polymer mortar for 7, 14, 21, and 28 days. The study's findings show that when the amount of polymer in a mortar increases, its compressive strength falls. The polymer mortar's compressive strength value, however, revealed the best outcomes after 28 days of immersion. The results of XRF characterization data, SiO_2 and CaO are the most common components in polymer mortar. Calcite, quartz, corundum, and hematite are the most prevalent phases. Results of SEM-EDS analysis display the polymer mortar's shape as well as the elements that were found, which include O, C, Ca, Si, Al, Fe, S, and Mg. Results from the FTIR characterization show wavelengths in the polymer mortar that correspond to the presence of functional groups such C-O, Si-O-Si, Si-O, and O-H.

Keywords: Cement mortar, PET plastic waste, EVA polymer, mechanical properties, physical properties

RASĀYAN *J. Chem.*, Vol. 18, No.2, 2025

INTRODUCTION

Over the past 170 years, mortar and concrete made with Portland cement have become popular construction materials.[1] Due to its popularity in the construction industry worldwide, mortar poses several environmental issues. One of them is the emission of greenhouse gases produced from the production of Portland cement, which is the raw material in mortar production, reaching 1.35 billion tons per year.[2] Furthermore, cement mortar still has several weaknesses, such as slow hardening, low tensile strength, significant drying shrinkage, and low resistance to chemicals. To address these issues, efforts can be made to modify mortar with polymers. This has been developed in several advanced countries. Polymer-modified mortar and concrete are considered promising construction options due to a good balance between performance impact and cost.[1] Of the 25 million tons of plastic produced in Europe annually, only 30% is recycled, while the rest is either incinerated or disposed of in landfills. Globally, it has been estimated that 86% of all plastic packaging is never collected or recycled.[3] Recycling waste is the best way to achieve sustainable plastic processing due to its environmental compatibility and economic benefits.[4] There are several types of plastic waste commonly found, such as High-Density Polyethylene (HDPE), Low-Density Polyethylene (LDPE), Linear Low-Density Polyethylene (LLDPE), nylon 6, Polystyrene (PS), Poly-Propylene (PP), Polyethylene Terephthalate (PET), and Polyvinyl Chloride (PVC).[5]

http://doi.org/10.31788/RJC.2025.1829147

Polyethylene Terephthalate (PET) is one of the most found thermoplastic polyesters on the market, in the form of bottles and food packaging. An economical way to recycle the polymer type Polyethylene Terephthalate (PET) is by using it as a substitute material in the construction industry, by using it as an aggregate mixed with cement.[6] As a result, PET used as aggregate in mortar and concrete formulations can enhance the sustainability of this waste with numerous positive impacts, such as reduced natural resource usage, waste consumption, environmental protection, and energy savings.[7] Besides PET, there are other polymers that can be used as substitute materials in mortar, such as Ethylene Vinyl Acetate (EVA). EVA is one of the polymers that enhance flexibility and bending strength[8], and the bonding strength of cement concrete.[9] Several researchers have used polymers in mortar mixtures. Abed et al., (2021) conducted a study by adding polyethylene terephthalate (PET) as a substitute for fine aggregate or sand in mortar.[10] The results of the compressive strength and flexural strength tests showed a decrease in the values of compressive strength and flexural strength starting with the addition of 15% PET. In the study conducted by Yeon et al., (2019), Ethylene Vinyl Acetate (EVA) in powder form was used as a substitution material.[11] The test results of the specimens indicated that at a curing age of 28 days, the compressive strength ranged from 32.92 MPa to 43.50 MPa, and the flexural strength ranged from 12.73 MPa to 14.49 MPa. The research results indicate that mortar modified with EVA polymer exhibits a high level of strength development, making the material advantageous for use in three-dimensional additive construction.

This work was carried out to investigate the effects on mechanical and physical characteristics of polymer mortar by combining cement and sand substitute materials, particularly EVA and PET polymers, based on prior investigations.

EXPERIMENTAL

Materials

In this study, the materials used include Portland cement, sand, Ethylene Vinyl Acetate (EVA) polymer, and Polyethylene Terephthalate (PET) polymer. These materials will undergo several characterizations, including chemical composition analysis, constituent phase identification, morphological characterization, and analysis of functional groups formed within the materials.

Methods

The parameters used in this experiment are shown in Table-1. Portland cement, sand, EVA, and PET are weighed according to the composition in Table-1. Then water is added, mixed, and cast into cubes measuring 5×5×5 cm^3. The specimens are left to stand for 24 h and then submerged for 7, 14, 21, and 28 days. The polymer mortar is then removed from the water, and testing is conducted on its mechanical and physical properties, including compressive strength, porosity, absorption, and density. Polymer mortar is also characterized using XRF, XRD, SEM-EDS, and FTIR. The compressive strength testing was conducted using a universal testing machine, type HT-2402. The chemical content analysis was performed using X-Ray Fluorescence with PanAnalytical Type Minipal 4 equipment, and phase structure analysis was conducted using X-Ray Diffraction with PanAnalytical Type Expertpro equipment. The morphology of the polymer mortar was obtained using Scanning Electron Microscopy Quattro S. Additionally, the functional groups formed were analyzed using Fourier Transform Infrared (FTIR) analysis with Bruker Type Invenio equipment.

Table-1 : Composition of Polymer Mortar

Sampel Code	Composition of material (%)				
	Cement	EVA	Sand	PET	Total
EVA/PET	20,0	0,0	80,00	0,00	100
2EVA/0,2PET	19,6	0,4	79,84	0,16	100
4EVA/0,5PET	19,2	0,8	79,60	0,40	100
6EVA/0,8PET	18,8	1,2	79,36	0,64	100
8EVA/1,1PET	18,4	1,6	79,12	0,88	100
10EVA/1,4PET	18,0	2,0	78,88	1,12	100

RESULTS AND DISCUSSION

Mechanical and Physical Tests

Figure-1(a) shows the graph of the compressive strength test results of polymer mortar after immersion. The results indicate that increasing the addition of EVA and PET polymers leads to a decrease in compressive strength values. This is proportional to the density values displayed in Fig.-1(b) The

decrease in density values in the polymer mortar may be due to the low density of the added polymer materials.[12] The values of absorption and porosity increase as shown in Fig.-1(c) and (d). This increase may occur because the shape of the polymer used as aggregate (PET) differs from sand.[13] Hence, it will form pores that increase the values of porosity and absorption in the polymer mortar.

Chemical Composition

Based on Table-1, there is an increase in the level of silica (SiO_2) found in boiler crust ash. Unextracted boiler crust ash has a silica (SiO_2) content of 38% and after extraction, the silica content is 96.1%. Based on the data obtained, it is known that through the silica extraction process using the sol gel method can increase the purity of silica compounds contained in boiler crust ash.

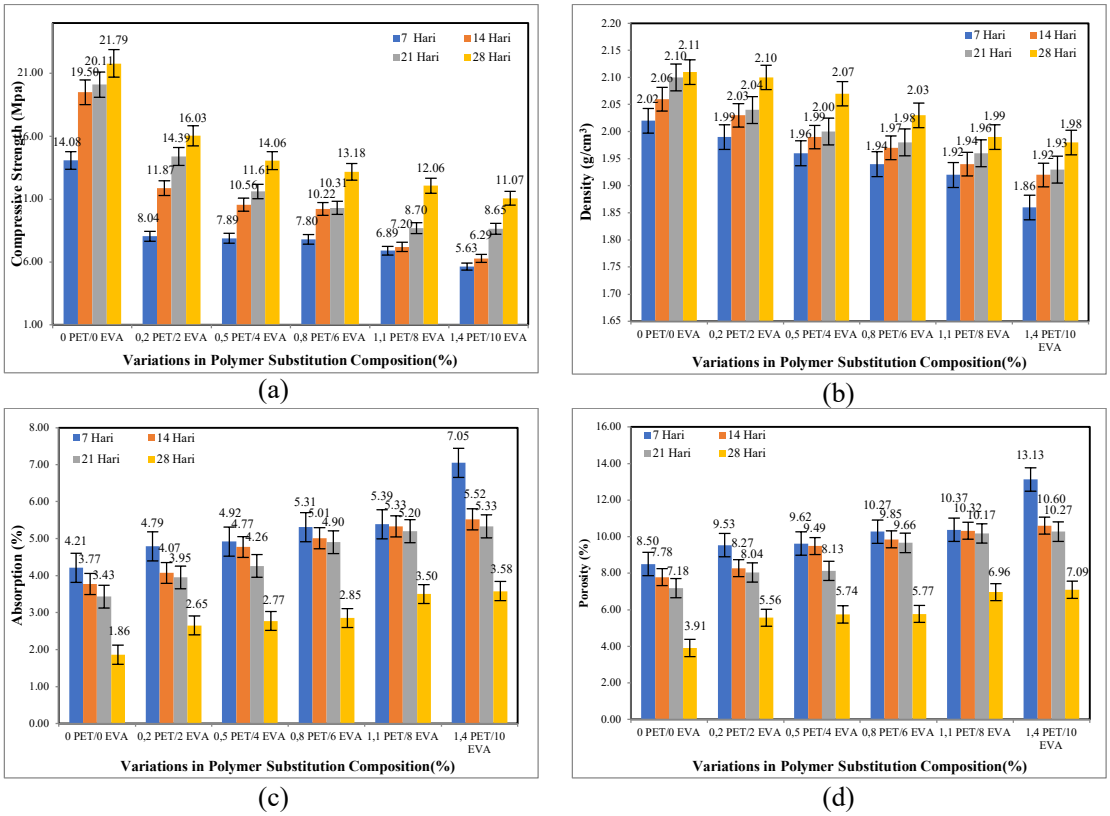

Fig.-1: (a) Compressive Strength, (b) Density, (c) Absorpstion, (d) Porosity

The high silica content indicates a relatively high level of purity in the extraction process. Portland cement has CaO compound as the highest content, amounting to 77.82%. Based on SNI 15-7064-2004, the CaO compound content that can be used as a building mixture is more than 45% and SO_3 less than 4%. The results of XRF characterization prove that the compound content in Portland cement raw materials can be used in this research as a raw material for making polymer mortar. SiO_2 is the most abundant compound in sand, accounting for 63.61%. Meanwhile, for EVA and PET polymers, after observation, the dominant content found is Ca. The complete chemical contents of the raw materials can be seen in Table-2 and Table-3. Based on Table-4, it can be observed that when the polymer mortar has been immersed, the dominant compounds formed are Calcium Oxide (CaO) and Silicon Dioxide (SiO_2). The characterization results of these samples follow the XRF analysis of raw materials such as Portland cement, sand, EVA, and PET.

Table-2: Chemical composition of cement and sand

Compounds (%wt)	SiO_2	CaO	Al_2O_3	Fe_2O_3	K_2O	TiO_2	SO_3	SrO	P_2O_5	ZrO_2
Portland Cement	9,49	77,82	2,91	5,94	1,29	0,42	1,59	0,29	-	-
Sand	63,61	1,73	17,12	6,39	8,97	0,87	-	-	0,64	0,20

Table-3: Chemical composition of polymer

Compounds (%wt)	Ca	Si	Sb	Fe	Er	K	Ti	Mn	Sc	Ni	Mg	Al
EVA	74,76	7,81	-	1,63	-	-	1,47	-	-	-	13,6	0,34
PET	57,61	-	14,58	11,59	8,28	4,69	2,1	0,43	0,43	0,29	-	-

Table-4: Chemical composition of polymer mortar

Oxide Compounds (%wt)	SiO_2	CaO	Al_2O_3	Fe_2O_3	K_2O	TiO_2	MgO	MnO	SrO	SO_3	BaO
7 Days	33,6	35,96	11,9	8,89	7,56	8,89	0,14	0,13	0,2	0,4	0,12
14 Days	30,3	38,65	11,35	9,5	7,01	9,5	1,19	0,11	0,25	0,35	0,14
21 Days	21,7	50,73	7,86	12,53	2,21	1,278	1,77	0,22	0,36	-	-
28 Days	22,3	47,97	8,18	13,68	2,48	1,35	1,62	0,22	0,36	-	-

XRD Analysis

Based on XRD analysis in Fig.-2, the characterization results of the raw materials exhibit diffraction patterns that can be classified into crystalline phases, marked by sharp phases with high intensity. In Fig.-2(a), the diffractogram of Portland cement shows the presence of the calcite ($CaCO_3$) phase, which has a rhombohedral crystal structure and represents the highest peak on the Portland cement diffractogram at 2θ=29.406°. Furthermore, for the hematite (Fe_2O_3) phase with a rhombohedral crystal structure, the highest intensity is at 2θ=33.115°. Meanwhile, the quartz (SiO_2) phase with a hexagonal crystal structure has the highest intensity at 2θ=26.652°. Based on this, it can be observed that all detected minerals show sharp peaks and good intensity, indicating the crystalline nature of each mineral component.[14]

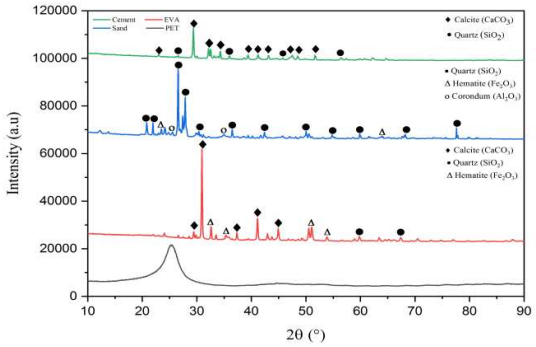

Fig. 1-. XRD of raw material (a) Portland Cement (b) Sand; (c) EVA; dan (d) PET

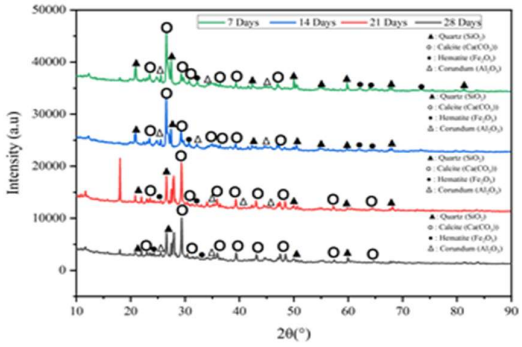

Fig. 3-. XRD of Polymer Mortar (a) 7 Days; (b) 14 Days; (c) 21 Days; and (d) 28 Days

Meanwhile, the diffractogram of sand can be seen in Fig.-2(b), which shows that the quartz (SiO_2) phase has a hexagonal crystal structure and represents the peak with the highest intensity in the sand diffractogram at 2θ=26.640°. Furthermore, for the corundum (Al_2O_3) phase with a rhombohedral crystal structure, the highest intensity is at 2θ=43.363°. The Al_2O_3 compound plays a significant role in the hardening process.[15] Another formed phase is hematite (Fe_2O_3) with a rhombohedral crystal structure, having the highest intensity at 2θ=33.115°. Meanwhile, the calcite ($CaCO_3$) phase has the highest intensity at 2θ=29.406° with a rhombohedral structure. In Fig.-2(c), the X-ray diffractogram of PET polymer derived from waste, specifically beverage bottles, is shown. The diffractogram displays a broad peak for the Polyethylene Terephthalate (PET) sample. This indicates that the material has an amorphous structure.[16] The diffractogram shows its highest hump at a diffraction angle (2θ) of 25.277°. This may be due to the rapid cooling rate during the PET sheet formation process. Consequently, the long molecular chains do not have sufficient time to rearrange into a crystalline phase at low temperatures.[17] Figure-2(d) shows the diffractogram of EVA. The calcite ($CaCO_3$) phase formed has a rhombohedral crystal structure and represents the highest peak in the sand diffractogram at 2θ=29.406°. For the quartz (SiO_2) phase with a hexagonal crystal structure, the highest intensity is at 2θ=26.640°. Meanwhile, the hematite (Fe_2O_3) phase has its highest intensity at 2θ=33.115°. Polyethylene is a semi-crystalline polymer, and the addition of VAA groups reduces its degree of crystallinity. The higher the VA group content, the lower the degree of crystallinity of the copolymer, and the copolymer becomes completely amorphous if the VA content exceeds 50%[9]. In Fig.-3(a), the diffractogram of polymer mortar with a soaking time of 21 days can be seen. The formation of the calcite ($CaCO_3$) phase, which

has a rhombohedral structure, shows the highest intensity at 2θ=29.406°. For the quartz (SiO_2) phase with a hexagonal crystal structure, the highest intensity is at 2θ=26.640°. The hexagonal crystal structure is composed of a tetrahedral arrangement formed between silicon and oxygen atoms that crystallize. The quartz phase influences the mechanical properties of the mortar due to the ability of quartz particles to create crack resistance.[15] Another phase that forms is corundum (Al_2O_3) with a rhombohedral structure, showing the highest intensity at 2θ=43.363°. Meanwhile, the hematite (Fe_2O_3) phase with a rhombohedral crystal structure has the highest intensity at 2θ=33.115°.
In addition, the diffractogram of polymer mortar with a soaking time of 28 days is shown in Fig.-3(b). The formation of the calcite ($CaCO_3$) phase, with a rhombohedral structure, has the highest intensity at 2θ=29.406°. For the quartz (SiO_2) phase with a hexagonal crystal structure, the highest intensity is at 2θ=26.640°. Nergis et al. (2020) stated that the SiO_2 compound influences the mechanical properties of a material.[15] Another phase that forms is corundum (Al_2O_3) with a rhombohedral structure, showing the highest intensity at 2θ=43.363° and playing an important role in the mortar hardening process. Meanwhile, the hematite (Fe_2O_3) phase with a rhombohedral crystal structure has the highest intensity at 2θ=33.115°. The characterization results with XRD align with the testing results using XRF, which state that the elements Ca, Si, Al, and Fe are the elements with the highest levels contained in the polymer mortar composition of 2% EVA and 0.2% PET, with CaO being the most dominant.

SEM-EDS Analysis
Figure-4 shows the morphology of raw materials with a magnification of 5000×. In Fig.-4(a), the dominant distribution of Ca and Si elements is observed in Portland cement material, with percentages of 29.34% and 4.51%, respectively. Figure-4(b) illustrates that Si and Al elements dominate the content of the sand material. As for EVA and PET polymers, the most dominant elements are Ca and Si. This aligns with the XRF results obtained from the raw materials.

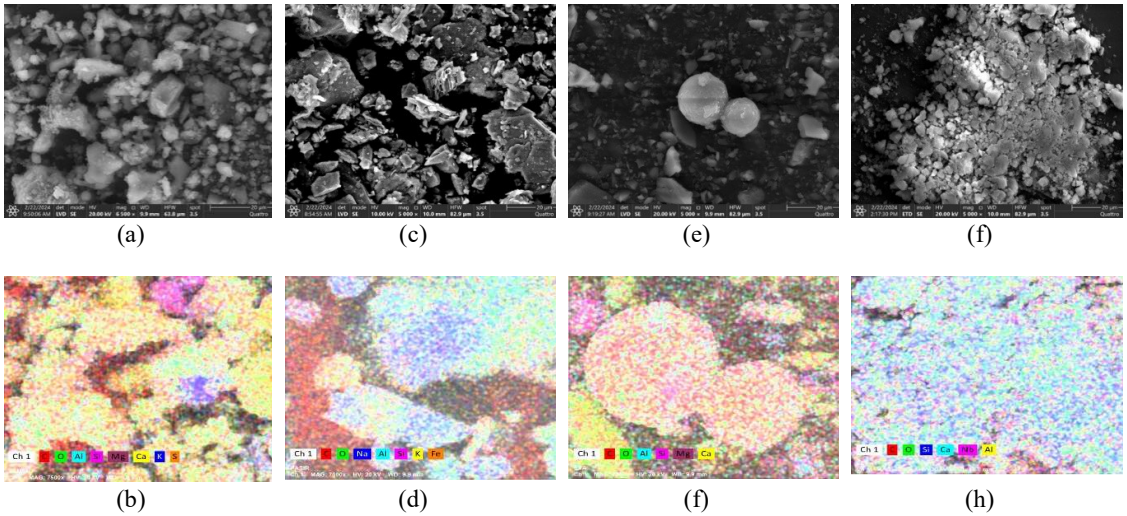

Fig. 4-. The results of SEM-EDS analysis show the Morphological Shapes and the Chemical Element Distribution Mapping of (a) (b) Portland Cement; (c) (d) Sand; (e) (f) EVA; and (g) (h) PET

The results of the SEM-EDS analysis on polymer mortar are shown in Fig.-5. The EDS results for each sample indicate that Ca and Si elements are the most dominant content in the polymer mortar. The polymer used as a substitute material in the mortar affects the pores in the formation of Calcium Silicate Hydrate (C-S-H).[18] The formation of Calcium Silicate Hydrate (C-S-H) occurs when a chemical reaction takes place between silica (Si) and calcium hydroxide $Ca(OH)_2$, reacting with water. Therefore, the longer the immersion time, the greater the influence on the C-S-H compound, which can provide strength and mechanical stability to the mortar.[19] This can be observed in Fig.-5, which shows that the pores in the polymer mortar decrease with increasing immersion time, resulting in the formation of more optimal bonds between cement and water.[18] In polymer mortar with a 28-day immersion time, the formation of ettringite (Aft) has also been observed, which appears as needle-like structures growing among some C-S-H.

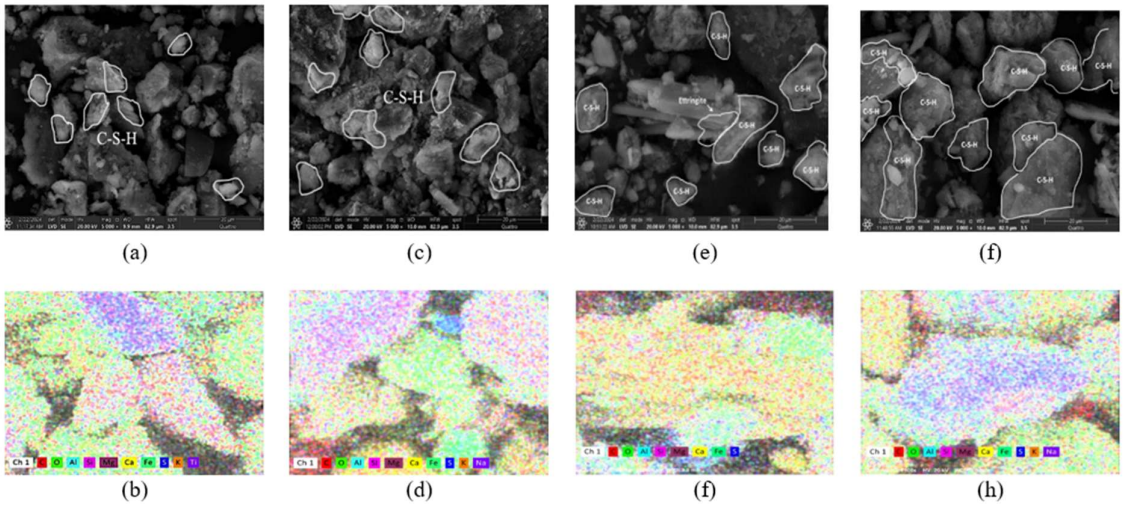

Fig. 5-. The results of SEM-EDS analysis show the Morphological Shapes and the Chemical Element Distribution Mapping of Polymer Mortar: (a) (b) 7 Days; (c) (d) 14 Days; (e) (f) 21 Days; and (g) (h) 28 Days

FTIR Analysis

FTIR characterization was conducted to determine the functional groups present in the raw materials and samples with the highest compressive strength based on their immersion time. Based on the graph in Fig.-6(a), functional groups and wavelength lengths of the raw cement materials can be observed. At a wavelength of 3400 cm^{-1}, there is an O-H bond, indicating a slight increase in water content. At wavelengths from 900 to 1000 cm^{-1}, strong asymmetric bending represents the formation of C-S-H in the mortar.[20] Figure-6(a) can indicate the functional groups of the sand raw material. At wavelengths of 999 cm-1 and 911 cm-1, Si-O bands are formed. At wavelengths of 759, 694, 645, and 530 cm^{-1}, Si-O-Si bands are formed.[21] Based on the graph in Fig.-6(b), it shows the results of FTIR analysis on the EVA polymer. The analysis results in the graph indicating wavelengths of 3365, 1730, and 605 cm^{-1} represent C=O functional group bonds. C-H functional groups are formed at wavelengths of 2933 and 2862 cm^{-1}. At wavelengths of 1230, 1093, and 1018 cm^{-1}, there are C-O functional groups. CH_3 bonds are formed at a wavelength of 1371 cm^{-1}. Wavelengths of 1430 and 728 cm^{-1} indicate the formation of CH_2 bands, showing the presence of absorption in ethylene groups.[22] Figure-6(c) shows the results of the FTIR analysis of the PET polymer. The graph of aliphatic C-H stretching exhibits a small peak at a wavelength of 2969 cm^{-1} and undergoes a similar peak bending at a wavelength of 972 cm^{-1}. The stretching band of the C=O ester group is located at a wavelength of 1714 cm^{-1}. Wavelengths of 1242 and 1091 cm-1 show two intense bands for the stretching of C-O-C in ester groups. The C=C functional group is indicated at 1407 cm^{-1}. At a wavelength of 1016 cm^{-1}, there is an absorption band caused by C-H bond bending. C-H bonds are indicated at a wavelength of 723 cm^{-1}.[23] An Analysis of functional groups was also conducted on the polymer mortar resulting from immersion. Based on Fig.-7, the wavelength and functional groups formed in the polymer mortar can be observed. The analysis results in the graph in Fig.-7(a) show that the polymer mortar with a 7-day immersion time exhibits wavelengths of 3693, 3694, and 3618 cm^{-1}, indicating stretching in the O-H band, which signifies the presence of adsorbed water molecules from the C-S-H phase. At a wavelength of 1645 cm^{-1}, there is a bond of the C=C functional group. The bond of the C=H functional group is indicated at wavelengths of 1416 and 1414 cm^{-1}.[24,25]

Based on the study conducted by Yu et al., (1999), they investigated the structure of C-S-H formed at wavelengths between 980 to 1080 cm^{-1}.[26] Figure-(b) shows strong asymmetric bending indicating the formation of C-S-H in the polymer mortar, as evidenced by the wavelengths of 1003 and 1000 cm^{-1}, which indicate stretching in the Si-O band.[24] At wavelengths of 911 and 908 cm^{-1}, there are Si-O functional group bonds. At wavelengths of 871 and 875 cm^{-1}, there are C-H functional group bonds. At wavelengths of 531 and 530 cm^{-1}, there are Si-O functional group bonds.[24,25,27-29] Figure-7(c) shows the wave numbers of the polymer mortar with a 21-day immersion time. Based on the analysis conducted, the formation of Calcium Silicate Hydrate (C-S-H) can be observed in the Si-O-Si band at a wavelength of 968 cm^{-1}. Another functional group formed is Si-O at a wavelength of 530 cm^{-1}.

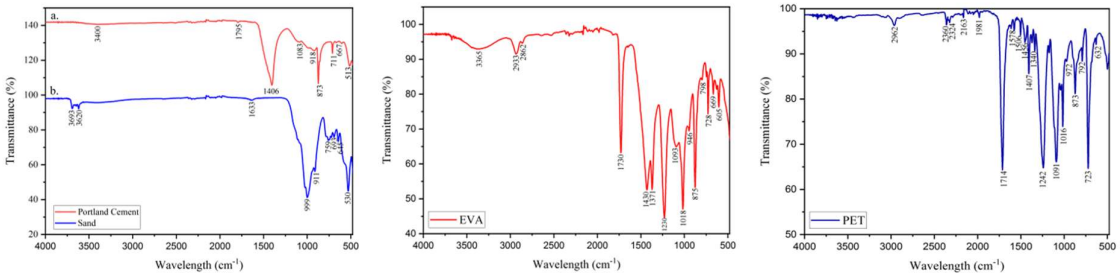

(a) (b) (c)

Fig.-6: Analysis FTIR of raw material (a) Cement and Sand (b) EVA (c) PET

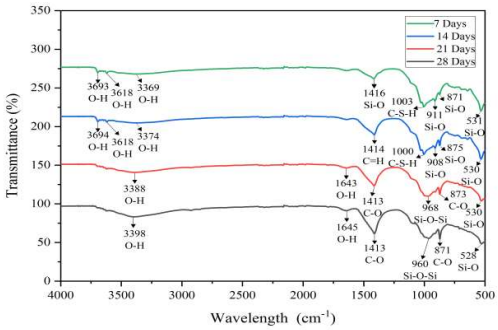

Fig.-7: FTIR Analysis of Polymer Mortar with Soaking Time (a) 7 Days; (b) 14 Days; (c) 21 Days; and (d) 28 Days

For wavelengths of 1643 and 3388 cm^{-1}, the O-H functional group is formed, indicating the presence of water molecules. The C-O band formed at wavelengths of 1413 cm^{-1} and 873 cm^{-1} represents the carbonate phase. Based on the graph in Fig.-7(d), the wavelengths formed in the polymer mortar with a 28-day immersion time can be observed. The Si-O-Si band can be marked as the formation of Calcium Silicate Hydrate (C-S-H) at a wavelength of 960 cm^{-1}. Another functional group formed is Si-O at a wavelength of 528 cm^{-1}. At wavelengths of 1645 cm^{-1} and 3398 cm^{-1}, the O-H functional group is formed, indicating the presence of water molecules adsorbed from the C-S-H phase. The C-O band at wavelengths of 1413 cm^{-1} and 871 cm^{-1} signifies the presence of the carbonate phase in the polymer mortar.[9,24,28]

CONCLUSION

The compressive strength values decrease with the increasing addition of EVA and PET polymers. The most optimal test results in the study are found in the polymer mortar with 0.2% PET and 2% EVA substitution (sample code 0.2 PET/2 EVA). After 28 days of immersion, it has the lowest absorption and porosity values of 2,65% and 5,56%, respectively, and the highest density and compressive strength values of 2,10 g/cm^3 and 16,03 MPa. The highest compressive strength value in the 0,2 PET/2 EVA sample code indicates that the polymer mortar in this study meets the requirements of SNI 03-6882-2002, as the mortar value exceeds 12,5 MPa, classifying it as type S mortar. The mortar contains dominant compounds of SiO_2, CaO, Fe_2O_3, and Al_2O_3, with formed phases including calcite, quartz, corundum, and hematite. SEM-EDS characterization of the polymer mortar indicates the most dominant distribution of Ca and Si elements. Additionally, FTIR characterization shows several wavelengths indicating the presence of functional groups C-O, Si-O-Si, Si-O, and O-H in the polymer mortar. The formation of Si-O-Si signifies strong asymmetric bending, indicating the formation of Calcium Silicate Hydrate (C-S-H).

ACKNOWLEDGMENTS

The first author is funded by DIPA-ORNM (Nanotechnology and Material Research Agency, National Research and Innovation Agency (BRIN-Indonesia), with grant number B-11575/III.10/TK.01.00/12/2023. The second author is funded by the Faculty of Mathematics and Natural Sciences, University of Indonesia under the Publication Grant scheme 2025.

CONFLICT OF INTERESTS

The authors declare that there is no conflict of interest.

AUTHOR CONTRIBUTIONS

All the authors contributed significantly to this manuscript, participated in reviewing/editing, and approved the final draft for publication. The research profile of the authors can be verified from their ORCID ids, given below:

Muhammad Amin https://orcid.org/0000-0001-5410-7303
Ariadne Lakshmidevi Juwono https://orcid.org/0000-0002-2068-9402
Sudibyo https://orcid.org/0000-0002-5493-1041
David Chandra Birawidha https://orcid.org/0000-0001-8279-7401
Sugeng Priyanto https://orcid.org/0000-0001-6570-1869
Muhammad Al Muttaqii https://orcid.org/0000-0001-5000-3478

REFERENCES

1. Y. Ohama, *Handbook of Polymer-Modified Concrete and Mortars: Properties and Process Technology*, New Jersey: Noyes Publications (1995).
2. D. Hardjito, S. E. Wallah, D. M. Sumajouw, B.V. Rangan, *Materials Journal*, **101(6)**, 467(2024), https://doi.org/10.14359/13485.
3. M.T. Letcher, *Plastic Waste and Recycling: Environmental Impact, Societal Issues, Prevention, And Solutions*, Elsevier Science. Netherlands, 2020.
4. M. Shamsuyeva, H.J. Endres, *Composites Part C: Open Access*, **6**, 1(2021), https://doi.org/10.1016/J.Jcomc.2021.100168.
5. J. Hopewell, R. Dvorak, E. Kosior, *Philosophical Transactions of The Royal Society B: Biological Sciences*, **364 (1526)**, 2115(2009), https://doi.org/10.1098/rstb.2008.0311.
6. S. Akçaözoğlu, C.D. Atiş, K. Akçaözoğlu, *Waste Management*, **30(2)**, 285(2010), https://doi.org/10.1016/J.Wasman.2009.09.033.
7. H.T. Mohan, K. Jayanarayanan, K.M. Mini, *Construction Building Material*, **271**, 121520(2021), https://doi.org/10.1016/j.conbuildmat.2020.121520.
8. C. Shi, X. Zou, P. Wang, *Construction And Building Materials,* **193**, 474(2018), https://doi.org/10.1016/J.Cemconcomp.2020.103821.
9. A. A. Mansu, O. L. Do Nascimento, H.S. Mansur, *Cement and Concrete Research*, **39(12),** 1199(2009), https://doi.org/10.1016/J.Cemconres.2009.07.020.
10. J. M. Abed, B.A. Khaleel, I. S. Aldabagh, N.M. Sor, *Journal of Physics: Conference Series*, **1973 (1)**, 1(2021), https://doi.org/10.1088/1742-6596/1973/1/012121.
11. K. S. Yeon, K. K. Kim, J. Yeon, H. J. Lee, *Materials*, **12(16)**, 1(2019), https://doi.org/10.3390/Ma12162600.
12. B. Mishra, R.S. Mishra, *International Journal Innovative Research Science Engineering Technolology*, **4(11)**, 11232(2015), https://doi.org/10.15680/Ijirset.2015.04110668.
13. C. Albano, N. Camacho, M. Hernández, A. Matheus, A.J.W.M. Gutierrez, *Waste Management*, **29(10)**, 2707(2009), https://doi.org/10.1016/J.Wasman.2009.05.007.
14. M. Amin, D.C. Birawidha, K. Isnugroho, M. Al Muttaqii, *Acta Polytechnica*, **59(6)**, 536(2019), https://doi.org/10.14311/AP.2019.59.0536.
15. D. B. Nergis, P. Vizureanu, L. Andrusca, D.C. Achitei, *IOP Conference Series: Materials Science and Engineering*, **572(1)**, 12026(2019), http://dx.doi.org/10.1088/1757-899X/572/1/012026.
16. R.A.X Nunes, V. C. Costa, V. M. D. A. Calado, J. R. T. Branco, *Materials Research*, **12**, 121(2009), http://dx.doi.org/10.1590/S1516-14392009000200002.
17. S. Park, S. Thanakkasaranee, H. Shin, Y. Lee, G. Tak, J. Seo, *Polymers*, **13(5),** 728(2021), https://doi.org/10.3390/polym13050728.
18. Y. Peng, G. Zhao, Y. Qi, Q. Zeng, *Cement and Concrete Composites*, **114**, 1(2020).
19. F. M. Lea, Lea's Chemistry of Cement and Concrete, Elsevier Science. United Kingdom, (2018).
20. M. Horgnies, J.J. Chen, C. Bouillon, *Wit Transaction Engineering Sciences*, **77**, 251(2013), https://doi.org/10.2495/MC130221.

21. B. H. Stuart, Infrared Spectroscopy: Fundamentals And Applications, John Wiley And Sons Ltd, United Kingdom, (2004).
22. L. J. Bellamy, The Infrared Spectra of Complex Molecules, Science Press, Beijing, **2**, (1975).
23. R. M. Silvertein, G. C. Bassler, T. C. Morril, Spectrometric Identification of Organic Compounds 4th Ed., John Wiley & Sons, New York, (1981).
24. D. A. D. Silva, H. R. Roman, P.J.P. Gleize, *Cement and Concrete Research*, **32(9)**, 1383(2002), https://doi.org/10.1016/S0008-8846(02)00805-0.
25. A. S. Benosman, M. Mouli, H. Taibi, Belbachir, Y. Senhadji, I. Behlouli, D. Houivet, *Progress in Rubber, Plastics and Recycling Technology*, **33(3)**, 139(2012), https://doi.org/10.1177/147776061703300304.
26. P. Yu, R. J. Kirkpatrick, B. Poe, P. F. Mcmillan, X. Cong, *Journal of American Ceramic Society*, **82**, 742(1999), https://doi.org/10.1111/J.1151-2916.1999.Tb01826.X.
27. M. O. Yusuf, *Applied Sciences*, **13(5)**, 1(2023), https://doi.org/10.3390/App13053353.
28. E. V. Tararushkin, T. N. Shchelokova, V. D. Kudryavtseva, *IOP Conf. Series: Material Sciences Engineering*, **919(2)**, 1(2020), https://doi.org/10.1088/1757-899x/919/2/022017.
29. V. S. Kashyap, U. Agrawal, K. Arora, G. Sancheti, *IOP Conference Series: Earth And Environmental Science*, **796(1)**, 1(2021), https://doi.org/10.1088/1755-1315/796/1/012022.

[RJC-9147/2024]